ELSEVIER

Journal of Chromatography A, 699 (1995) 297–313

JOURNAL OF CHROMATOGRAPHY A

Wall adsorption in capillary electrophoresis Experimental study and computer simulation

Sergey V. Ermakov[1], Michael Yu. Zhukov[2], Laura Capelli, Pier Giorgio Righetti*

Department of Cell Biology, University of Calabria, 87030 Arcavacata di Rende (Cosenza), Italy

First received 2 August 1994; revised manuscript received 6 December 1994; accepted 14 December 1994

Abstract

A semi-quantitative model based on non-linear equilibrium chromatography coupled with diffusion-driven sample sorption at the wall was developed to account for and predict potential binding of an analyte to the wall in capillary electrophoresis. It was then used for computer simulation of sample concentration profiles corresponding to different experimental conditions (sorption kinetics, capillary length, wall capacity and initial sample concentration). The binding phenomena were also studied experimentally by means of analysis of the sample peak shape (including peak height and area). Contrary to expectations, it was found that the interaction of small monovalent cations with the charged capillary wall does not lead to strong adsorption, as the sample mass is not lost during experiment and the peak shape remains close to that which one could expect in the absence of interaction. For polycations (e.g., poly-L-histidine) at any pH above 3, sample adsorption is evident by a lack of return of the baseline to zero, after peak passage, with progressively higher levels at progressively increasing buffer pH values. Upon several runs with a polycation, the surface charge on the wall changes from negative to positive, as evidenced by reversal of electroosmotic flow. However, it was discovered that even under these last conditions, the sample–wall interaction was rather strong. The influence of NaOH washing and the addition of different substances (urea, Tween-20, sodium chloride) on adsorption was studied. The comparison between simulated results and experimental data is discussed.

1. Introduction

High-performance capillary electrophoresis (HPCE) was developed as a very fast and efficient separation method for different applications [1,2]. Although in the last decade its capabilities have been substantially extended, there is still considerable potential for further growth (see, e.g., [3–5]). However, despite the advantages, there are some obstacles leading to loss of separation power, such as sample adsorption on the capillary wall. This problem is especially severe for high-molecular-mass substances such as proteins, polypeptides and DNA [6]. Most separations are performed in fused-silica capillaries having inner surfaces that become charged in electrolyte solutions and could potentially interact with sample species by means of electrostatic attraction. There are several ways

* Corresponding author. Address for correspondence: Via Fratelli Cervi No. 93, Segrate 20090 (Milan), Italy.

[1] Permanent address: Keldysh Institute of Applied Mathematics, Russian Academy of Sciences, Miusskaya Sq. 4, Moscow 125047, Russian Federation.

[2] Permanent address: Rostov State University, Zorge St. 5, Rostov-na-Donu 344104, Russian Federation.

0021-9673/95/$09.50
SSDI 0021-9673(94)01228-8

to reduce ionic interactions. The most popular and probably the most effective is long-term coating of the capillary inner surface with different polymers [7–10]. Another way to prevent sample adsorption is to create a so-called dynamic coating by adding some substances to the buffer solution that compete with samples for cation-exchange sites on the wall. Different additives have been tried for this purpose: alkali metal cations [11], metal amine complexes of bivalent cations [12], amines [13] and zwitterions [14]. The third way of modulating the sample adsorption is to control the wall potential by means of an external electric field [15,16], but currently this option is not available on commercial units. Finally, the simplest way to avoid strong interaction is to use buffers at pH extremes, in which either the ionization of silanols is suppressed or the separation is performed at a pH above the isoelectric points of proteins.

Other possible sample adsorption mechanisms are hydrophobic and hydrogen bond interactions. A protein, when attached to the wall, could neutralize its electric charge (at least partially), which in turn could potentially lead to an increase in its hydrophobicity with further adhesion to the wall via sample–sample interaction. Undissociated hydroxyl groups can also form the hydrogen bonds with sample substances. These two kinds of interactions may occur also in coated capillaries [17].

The wall–sample interaction leads not only to degradation of resolution, but also to sample loss. In an uncoated capillary it could be partially or completely adsorbed at the beginning of the capillary [18]. This in turn could lead to non-uniformities of charge density on the inner capillary wall and, hence, to non-uniform electroosmotic flow, which causes additional sample dispersion [18,19].

A mathematical model describing in detail the adsorption dynamics is still not available owing to lack of knowledge about this process. Existing models assume a chromatographic mechanism of interaction [20,21] with linear sorption kinetics. Similar equations with the same or other kinetics, as previously applied to chromatography, have been studied [22–24]. In electrophoresis, instead of solving the full set of equations, the loss of resolution is usually estimated by means of plate height theory as a function of column capacity factor [20,21,25,26]. However, the papers cited do not provide any comparison with experimental data.

In this work, we studied the sample interaction with the capillary wall both experimentally and by means of computer simulation. The evolution of the sample zone under different conditions was observed and the experimental chromatograms were compared with the simulated chromatograms. Two migration modes were tried: a normal electrophoretic run under the impact of an electric field and a pressure run in which the sample was carried by a pressure-driven flow, i.e., similar to a chromatographic separation mode. The analysis of the experimental data with the help of computer simulation is presented.

2. Theory

Our mathematical model is based on nonlinear equilibrium chromatography in which the exchange of bound sample with the liquid phase is described by kinetic equations [20,22,27]. This model is updated by including into consideration the sample transport by means of electric field while accounting for interaction between sample species and background electrolyte due to the dependence of conductivity on sample concentration. By using the averaging method it is possible to construct a set of equations which are complete and self-sufficient.

Let us suppose that the electrolyte solution is placed in a thin cylindrical capillary that is long compared with its inner radius r_0. We assume that the processes of adsorption–desorption are taking place at the boundary of a thin layer with depth d adjacent to the inner capillary surface. These processes are described by kinetic equations [24]:

$$-\left\{\frac{\partial a}{\partial t}\right\}_{\text{exch}} = \left\{\frac{\partial q}{\partial t}\right\}_{\text{exch}} = k_a(S-q)a - k_d q, \quad r = r_0 - d \tag{1}$$

where a is the sample concentration in the liquid phase (i.e. in the region $0 \leq r \leq r_0 - d$), q is the concentration of sample attached to the wall (i.e. in the region $r_0 - d \leq r \leq r_0$), S is the capacity of adsorbing layer, k_a and k_d are the coefficients of adsorption and desorption, respectively, and "exch" signifies exchange.

2.1. Equation for adsorbing layer

The sample interaction with the wall is followed by its diffusion into a layer of thickness d. The inner surface of the capillary $r = r_0$ is considered to be impermeable to the substance, so the diffusion in the adsorbing layer is described by the equation

$$\frac{\partial q}{\partial t} = \delta \Delta_r q, \quad r_0 - d \leq r \leq r_0 \tag{2}$$

with the boundary condition at capillary surface

$$-\delta \cdot \left.\frac{\partial q}{\partial r}\right|_{r=r_0} = 0 \tag{3}$$

where δ is the diffusion coefficient in the adsorbing layer and Δ_r is the Laplacian in a cylindrical coordinate system:

$$\Delta_r = \frac{1}{r} \cdot \frac{\partial}{\partial r} \cdot r \frac{\partial}{\partial r} \tag{4}$$

The problem (2)–(3) should be completed by a boundary condition at $r = r_0 - d$. This condition will be derived further from the mass conservation law.

2.2. Equation for the liquid phase

The sample transport processes in the capillary are described by the equation

$$\frac{\partial a}{\partial t} + \frac{\partial i}{\partial z} - \epsilon \Delta_r a = 0, \quad 0 < r \leq r_0 - d \tag{5}$$

with the condition at the infinity and at the capillary axis

$$i|_{z=\pm\infty} = 0, \left.\frac{\partial a}{\partial r}\right|_{r=0} < \infty \tag{6}$$

where i is the substance flux density in the direction z along the capillary axis and ϵ is the diffusion coefficient along axis r. The sample transport is caused by diffusion, electromigration or pressure-driven flow, so its flux is

$$i = \kappa_1 \mu E a + \kappa_2 v_p a - D \cdot \frac{\partial a}{\partial z} \tag{7}$$

where μ is the mobility, E is the intensity of the electric field, D is the diffusion coefficient in the solution along axis z and $v_p = v_p(r)$ is the velocity of pressure-driven flow, if an external pressure difference is applied; the parameters κ_1 and κ_2 have values either 1 and 0 or 0 and 1, respectively, which means that only one of two transport mechanisms at a time could be operative during a particular run. Thus, if the electric field is applied the pressure could not be applied, and vice versa. Two different diffusion coefficients in directions r and z were introduced, because in fact they describe different processes. Further, by means of averaging along the radial direction, the coefficient ϵ will be eliminated from the model while the coefficient D will describe the overall dispersion in the z direction, i.e., diffusion and convective transport together (see, e.g., [28,29]). The current density j is expressed by Ohm's law:

$$j = \sigma E, \quad \sigma = \sigma_0(1 + \alpha a) \tag{8}$$

where σ is the electrolyte conductivity, σ_0 is the conductivity of a "pure" buffer and α is a constant coefficient accounting for the electrophoretic interaction between sample and buffer. The Eq. 7 is then rewritten as

$$i = \kappa_1 \cdot \frac{\mu E_0 a}{1 + \alpha a} + \kappa_2 v_p a - D \cdot \frac{\partial a}{\partial z}, \quad E_0 = \frac{j}{\sigma_0} \tag{9}$$

2.3. Equation for the averaged concentration

Let us define by $\langle f \rangle$, as customary, the averaged value of the function $f(r, z, t)$ within a capillary (i.e., for the region $0 \leq r \leq r_0 - d$) as

$$\langle f \rangle = \langle f \rangle(z, t) = \frac{1}{\pi(r_0 - d)^2} \int_0^{2\pi} d\phi \int_0^{r_0 - d} f(r, z, t) r \, dr,$$
$$c = \langle a \rangle \tag{10}$$

where c is the averaged concentration.

By integrating Eqs. 5 and 9 with respect to r from 0 to $r_0 - d$, we derive

$$\frac{\partial c}{\partial t} + \frac{\partial \langle i \rangle}{\partial z} = \frac{2\epsilon}{r_0 - d} \cdot \left.\frac{\partial a}{\partial r}\right|_{r=r_0-d} \tag{11}$$

$$\langle i \rangle = \left\langle \kappa_1 \cdot \frac{\mu E_0 a}{1 + \alpha a} + \kappa_2 v_p a - D \cdot \frac{\partial a}{\partial z} \right\rangle \approx \kappa_1 \cdot \frac{\mu E_0 c}{1 + \alpha c} + \kappa_2 \bar{v}_p c - D \cdot \frac{\partial c}{\partial z} \tag{12}$$

By defining the averaged flux $\langle i \rangle$, we neglect the deviation of concentration a and take the concentration c averaged in the radial coordinate. In addition, it is necessary to define the concentration flux $[-\epsilon(\partial a/\partial r)|_{r=r_0-d}]$. We assume that this flux is given as (compare with Eq. 1)

$$-\epsilon \cdot \left.\frac{\partial a}{\partial r}\right|_{r=r_0-d} = d[k_a(S - q)c - k_d q] \equiv G\,, \quad r = r_0 - d \tag{13}$$

where G is the source of the substance a and q at the boundary of adsorbing layer. Note that we changed the concentration a by the averaged concentration c in Eq. 1.

Finally, the set of equations is written as

$$\frac{\partial q}{\partial t} = \delta \Delta_r q\,, \quad r_0 - d \leq r \leq r_0 \tag{14}$$

$$\frac{\partial c}{\partial t} + \frac{\partial}{\partial z}\left(\kappa_1 \cdot \frac{\mu E_0 c}{1 + \alpha c} + \kappa_2 \bar{v}_p c - D \cdot \frac{\partial c}{\partial z}\right) = \frac{2\epsilon}{r_0 - d} \cdot \left.\frac{\partial a}{\partial r}\right|_{r=r_0-d} \quad 0 < r \leq r_0 - d \tag{15}$$

$$-\epsilon \cdot \left.\frac{\partial a}{\partial r}\right|_{r=r_0-d} = d[k_a(S - q)c - k_d q] \equiv G\,, \quad r = r_0 - d \tag{16}$$

with the boundary condition and condition at infinity

$$-\delta \cdot \left.\frac{\partial q}{\partial r}\right|_{r=r_0} = 0,\ \langle i \rangle|_{z=\pm\infty} \equiv \left(\kappa_1 \cdot \frac{\mu E_0 c}{1 + \alpha c} + \kappa_2 \bar{v}_p c - D \cdot \frac{\partial c}{\partial z}\right)\Big|_{z=\pm\infty} = 0 \tag{17}$$

2.4. Boundary condition at $r = r_0 - d$

In order to derive the boundary condition for q at $r = r_0 - d$, we use the mass conservation law. By integrating Eqs. 14 and 15 in the domain $-\infty \leq z \leq +\infty$, $0 \leq r \leq r_0$, we obtain

$$\frac{\mathrm{d}}{\mathrm{d}t}\int_{-\infty}^{-\infty} \mathrm{d}z \int_{r_0-d}^{r_0} qr\,\mathrm{d}r = \int_{-\infty}^{+\infty} \mathrm{d}z \int_{r_0-d}^{r_0} \delta \cdot \frac{1}{r} \cdot \frac{\partial}{\partial r} \cdot r \cdot \frac{\partial q}{\partial r} \cdot r\,\mathrm{d}r \tag{18}$$

$$\frac{\mathrm{d}}{\mathrm{d}t}\int_{-\infty}^{+\infty} \mathrm{d}z \int_{0}^{r_0-d} cr\,\mathrm{d}r = -\int_{-\infty}^{+\infty} \mathrm{d}z \int_{0}^{r_0-d} \frac{\partial \langle i \rangle}{\partial z} \cdot r\,\mathrm{d}r + \int_{-\infty}^{+\infty} \mathrm{d}z \int_{0}^{r_0-d} \frac{2\epsilon}{r_0 - d} \cdot \left.\frac{\partial a}{\partial r}\right|_{r=r_0-d} r\,\mathrm{d}r \tag{19}$$

It is assumed that the sample substance with averaged concentration c (i.e., liquid phase) is located in the region $0 \leq r \leq r_0 - d$, whereas the substance with concentration q is contained within the solid phase $r_0 - d \leq r \leq r_0$.

The total sample mass is introduced by the following relationship:

$$M = \int_{-\infty}^{-\infty} \mathrm{d}z \int_{0}^{r_0} (c + q) r\,\mathrm{d}r = \int_{-\infty}^{+\infty} \mathrm{d}z \left(\int_{0}^{r_0-d} cr\,\mathrm{d}r + \int_{r_0-d}^{r_0} qr\,\mathrm{d}r\right)$$

Here the integration is fulfilled over the whole internal region of the capillary $0 \leq r \leq r_0$, but we assume that c is non-zero only within the region $0 \leq r \leq r_0 - d$, the same being valid for q in the region $r_0 - d \leq r \leq r_0$. Let us recall here the conservation of mass, that is,

$$\frac{\mathrm{d}M}{\mathrm{d}t} = 0$$

Then, by summing Eqs. 18 and 19, we have

$$0 = \frac{\mathrm{d}M}{\mathrm{d}t} = -\int_{-\infty}^{-\infty} \mathrm{d}z \int_{0}^{r_0-d} \frac{\partial \langle i \rangle}{\partial z} r\,\mathrm{d}r + \int_{-\infty}^{+\infty} \mathrm{d}z \int_{0}^{r_0-d} \frac{2\epsilon}{r_0 - d} \cdot \left.\frac{\partial a}{\partial r}\right|_{r=r_0-d} r\,\mathrm{d}r$$

$$+\int_{-\infty}^{+\infty} dz \int_{r_0-d}^{r_0} \delta \cdot \frac{1}{r} \cdot \frac{\partial}{\partial r} \cdot r \cdot \frac{\partial q}{\partial r} \cdot r \, dr$$

$$= -\int_0^{r_0-d} \langle i \rangle \Big|_{z=-\infty}^{z=+\infty} r \, dr$$

$$+\int_{-\infty}^{+\infty} dz \left(\int_{r_0-d}^{r_0} \delta \cdot \frac{1}{r} \cdot \frac{\partial}{\partial r} \cdot r \cdot \frac{\partial q}{\partial r} \cdot r \, dr \right.$$

$$\left. + \int_0^{r_0-d} \frac{2\varepsilon}{r_0 - d} \cdot \frac{\partial a}{\partial r}\Big|_{r=r_0-d} r \, dr \right) \quad (20)$$

It is obvious that the mass flux vanishes at infinity (see Eq. 17). Then, for mass conservation, it is sufficient to demand that the second term in Eq. 20 will disappear:

$$\int_{r_0-d}^{r_0} \delta \cdot \frac{1}{r} \cdot \frac{\partial}{\partial r} \cdot r \cdot \frac{\partial q}{\partial r} \cdot r \, dr +$$

$$\int_0^{r_0-d} \frac{2\epsilon}{r_0 - d} \cdot \frac{\partial a}{\partial r}\Big|_{r=r_0-d} r \, dr = 0$$

The last relationship allows us to derive the second boundary condition by means of its integration:

$$\delta \cdot \frac{\partial q}{\partial r}\Big|_{r=r_0-d} = \epsilon \cdot \frac{\partial a}{\partial r}\Big|_{r=r_0-d} \quad (21)$$

The condition 21 and Eq. 16 relate together Eqs. 14 and 15.

The detailed mathematics for deriving Eq. 21 are presented because usually this condition is obtained in a phenomenological way [27], by introducing the relationship between the volumes of a mobile and a stationary phase and the interface surface. These conditions could be inconsistent with the mass conservation law and require the introduction of free parameters.

2.5. Preliminary analysis of the model

The present mathematical model contains several parameters that are difficult to derive from experiments, e.g., coefficients of adsorption and desorption k_a and k_d, the capacity of the adsorbing layer S and its depth d and also the diffusion coefficient δ in this layer. The diffusion coefficient in the liquid phase D and a parameter α, characterizing the interaction of the sample with the background electrolyte, are much easier to determine.

The aim of this work was a computer simulation for a variety of parameters, k_a, k_d, S, α etc. Qualitative comparison of simulated concentration profiles with experimental data will help further to establish the correspondence between the parameters of the model and appropriate physical effects.

It is clear that an increase in adsorption coefficient k_a will lead to an increase in the amount of substance attached to the wall, whereas an increase of k_d will produce the opposite effect. However, within the limits of this model, it is impossible to predict what particular mechanism (ionic interaction, hydrophobic interaction or others) is responsible for attaching the sample to the wall. The parameter S characterizes the number of active adsorbing sites, which potentially could append the sample species from the liquid phase to the wall. The binding process takes place on the boundary $r = r_0 - d$. Owing to sample diffusion into a layer, these active sites become free and the adsorbed substance moves into a layer with depth d. In fact, this layer is imaginary and is characterized by three parameters. The "capacity" of the layer depends on S and d, whereas the rate of the processes taking place within the layer is determined by the diffusion coefficient δ.

2.6. Transition to dimensionless variables

In order to reduce the number of parameters and for the sake of convenience in simulations, it is better to go to dimensionless variables, which for the moment will be marked by a prime. Let us introduce L and $\mathcal{T}$ as a length and time scales, which are specified as follows:

$$t = t'\mathcal{T}, k_d' = \frac{d}{r_0} k_d \mathcal{T}, k_a' = \frac{d}{r_0} k_a \bar{C} \mathcal{T}, z = Lz',$$

$$d = r_0 d', r = r_0 r', S = \bar{C} S'$$

$$D' = \frac{D\mathcal{T}}{L^2}, \delta' = \frac{\delta \mathcal{T}}{r_0^2}, q = q'\bar{C}, c = c'\bar{C},$$

$$\alpha' = \alpha \bar{C}, v' = \frac{\mathcal{T} \mu E_0}{L} \quad \text{or} \quad v' = \frac{\mathcal{T} \bar{v}_p}{L} \quad (22)$$

where v' is a characteristic dimensionless velocity of a sample motion under the impact of an electric field or under a pressure difference and $\bar{C}$ is the characteristic concentration, e.g., initial sample concentration. The time scale may be

chosen in different ways, for example, by assuming that $v' = 1$, we obtain

$$\mathcal{T} = \frac{L}{\mu E_0} \text{ for } k_1 = 1,\ k_2 = 0,$$

$$\text{or} \quad \mathcal{T} = \frac{L}{\bar{v}_p} \text{ for } k_1 = 0,\ k_2 = 1 \tag{23}$$

Note that it is also possible to let $k'_d = 1$, then the time scale will be

$$\mathcal{T} = \frac{1}{k_d} \tag{24}$$

The first variant is preferable since in this case $\mathcal{T}$ is expressed through the known parameters L, μ, E_0 or $\bar{v}_p$ (usually we chose $L = 20L_i$, where L_i is the length of the injected sample plug), whereas in the case of Eq. 24 it is defined versus the coefficient k_d, which is difficult to determine.

Finally, the set of equations expressed in dimensionless variables is written as (the accents are now omitted)

$$\frac{\partial q}{\partial t} = \delta \cdot \frac{1}{r} \cdot \frac{\partial}{\partial r} \cdot r \cdot \frac{\partial q}{\partial r},\ 1 - d \leq r \leq 1,\ q = q(r, z, t) \tag{25}$$

$$-\delta \cdot \left.\frac{\partial q}{\partial r}\right|_{r=1} = 0,\ -\delta \cdot \left.\frac{\partial q}{\partial r}\right|_{r=1-d} = G\Big|_{r=1-d} \tag{26}$$

$$\frac{\partial c}{\partial t} + \frac{\partial}{\partial z}\left(\kappa_1 \cdot \frac{c}{1 + \alpha c} + \kappa_2 c - D \cdot \frac{\partial c}{\partial z}\right) = -\frac{2}{1-d} \cdot G\Big|_{r=1-d},\quad c = c(z, t) \tag{27}$$

$$\left(\kappa_1 \cdot \frac{c}{1 + \alpha c} + \kappa_2 c - D \cdot \frac{\partial c}{\partial z}\right)\Big|_{z=\pm\infty} = 0 \tag{28}$$

$$G = k_a(S - q)c - k_d q \tag{29}$$

2.7. Numerical algorithm

The solution of the set of Eqs. 25–29 for the general case is possible only with the help of numerical integration. In our work, for this purpose we used finite-difference methods, the true differential equations being replaced by a set of algebraic equations. The principal difficulty is the solution of the partial differential Eq. 27 describing the transport of a sample in the liquid phase. This equation is non-linear, since the migration velocity depends on sample concentration. The second difficulty is caused by the small coefficient D in the second derivative due to the small diffusion coefficient of the sample substance. The standard numerical methods could offer a satisfactory solution of this equation only if very fine space discretization with a small space increment is implemented [30]. Otherwise, the numerical solution could be distorted by false effects such as numerical diffusion and dispersion, which may completely obscure the details of the concentration profiles. In this work, for solving Eq. 27, we used a method previously developed [30] that proved efficient for simulating capillary electrophoresis [30,31]. Eq. 25 is a linear diffusion equation. However, the boundary condition 26 is non-linear, since it contains the function $c(z, t)$, which depends on concentration $q(r, z, t)$ on the boundary $r = r_0 - d$. Usually the solution of such equations does not cause great difficulties; one of the standard finite-difference methods [32] may be used for this purpose. The input data for a simulation are the initial concentration profiles in the mobile phase and in the adsorbing layer and the dimensionless parameters describing the properties of the system: adsorption and desorption coefficients k_a and k_d, diffusion coefficients D and δ, capacity of the wall S and its depth d, etc. The results of simulations could be presented in the form of the concentration distribution in solution and the adsorbing layer at any moment in time.

3. Experimental

3.1. Chemicals

All the chemicals were of analytical-reagent grade. Immobiline pK 9.3 was obtained from Pharmacia–LKB (Uppsala, Sweden), Poly-L-histidine from Sigma (St. Louis, MO, USA) and Tween-20 from Bio-Rad Labs. (Richmond, CA, USA). The other substances were purchased from Merck (Darmstadt, Germany).

3.2. Apparatus

Experiments were performed on a Beckman (Palo Alto, CA, USA) P/ACE System 2100 running under GOLD Software (Beckman). We used untreated fused-silica capillaries of I.D. 75 and 100 μm (Polymicro Technologies, Phoenix, AZ, USA) and total length 26.2 cm with a distance between the inlet and detection points of 19.4 cm. The absorbance was measured at 254 nm for pyridine and Immobiline and at 200 nm for other substances. Most experiments were performed in the voltage-stabilized regime with $V = 5$ or 10 kV. The temperature of the liquid-cooled capillary was maintained at 25°C. The samples were injected by application of an excess pressure of 0.5 p.s.i. or electrokinetically with the same voltage used during the run. Usually, between runs, the capillary was washed for 5 min consecutively with 1 *M* NaOH, 1 *M* HCl and water and finally for 15 min with buffer. In some cases, specified in the text, the capillary was washed only with buffer.

Computer modelling was performed using an IBM AT personal computer.

4. Results

Before starting the studies of the interaction of the sample with the wall, it is necessary to specify the criteria according to which this phenomenon will be determined and evaluated. The first is the direct comparison of the experimental UV profiles with theoretical concentration profiles. However, here it is possible only at a qualitative level because some parameters (k_a, k_b, S) are not known and only their hypothetical values could be used. For quasi-Gaussian profiles the estimation of sample interaction is possible by means of plate height theory when the theoretical value of peak dispersion is compared with the experimental value. The second criterion that could demonstrate a potential interaction is the loss of sample mass in the peak. This criterion is applied when the interaction is irreversible or at least the desorption process is slow. Finally, a baseline shift after sample passage could be taken as an indication of interaction. In our work we studied the sample interaction using two different sample migration modes: normal electrophoretic migration and pressure migration, in which the electric field is not applied and the sample moves together with the buffer, driven by the pressure difference.

4.1. Computer simulations

The solution of the set of Eqs. 25–29 depends on many parameters which could be considered as free parameters, i.e., their values are not known precisely and could change within wide limits. Because of this, we considered the influence of only a few parameters on the sample profiles while the others had fixed values. These include $\delta = 0.5$ and $d = 0.1$. The initial sample distribution was a rectangular sample plug of length 0.05 and $c_0 = 1$ in all cases unless other values are specified. These parameters assume fairly rapid diffusion in the adsorbing layer, which we suppose will occur in real cases when such a layer is thin. The input parameters for simulations are summarized in Table 1.

Table 1
Input parameters for simulations

Fig.	k_d	k_a	S	α	x_{det}	D	c_0
1	0.05–100	3	0.5	0	0.6	10^{-4}	1
2	0.05–100	5	0.5	−0.3	0.6	$2 \cdot 10^{-4}$	1
3	1	3	0.01–3	0	0.6	10^{-4}	1
4	1	3	1	0	0.6–1.5	10^{-4}	1
5	0.2	3	1	0	0.6	10^{-4}	0.2–1

The first series of simulations demonstrate the influence of adsorption–desorption kinetics. Temporal apparent concentration profiles c^* for several k_d values are presented in Fig. 1. This apparent concentration is connected with sample concentration in solution and on the wall by the equation

$$c^* = (r_0 - d)^2 c + [r_0^2 - (r_0 - d)^2]q.$$

It somehow models the detector response in real capillary units since both the sample in solution and the sample bound to the wall contribute to the total signal. The parameter α is set to zero, which, when $\kappa_1 = 1$ and $\kappa_2 = 0$, corresponds to a low sample concentration or, when $\kappa_1 = 0$ and $\kappa_2 = 1$, to a pressure-driven run. In both cases, in the absence of sample binding to the wall, the profile should be Gaussian. At very high desorption coefficients ($k_d = 100$), the sample interaction with the wall does not produce any visible effect on the profile. However at $k_d = 10$, i.e., when the desorption coefficient still exceeds three times that of adsorption, the effect of sample binding gives a noticeable tailing and decreases the number of theoretical plates by a factor $2.76 \cdot 10^3 / 1.18 \cdot 10^3 \approx 2.33$ (see Table 2). When the adsorption and desorption coefficients are equal, the loss in theoretical plates is more than tenfold. Further decrements in desorption rate give strongly tailing profiles, which, at $k_d = 0.05$, exhibit almost irreversible sample binding, when the baseline remains higher after the passage of a peak and does not go back to its previous value. Similar features are observed when sample interaction with the background electrolyte is observed ($\alpha = -0.3$, Fig. 2). It is interesting that at $k_d \rightarrow 0$ the electropherogram shape approaches its limiting shape.

Table 2
Influence of desorption coefficient on the number of theoretical plates

k_d	σ^2	N	Skew
No interaction	$3.4 \cdot 10^{-4}$	$2.94 \cdot 10^3$	$3 \cdot 10^{-3}$
100	$3.62 \cdot 10^{-4}$	$2.76 \cdot 10^3$	$1.03 \cdot 10^{-1}$
10	$8.44 \cdot 10^{-4}$	$1.18 \cdot 10^3$	1.396
3	$4.23 \cdot 10^{-3}$	$2.36 \cdot 10^2$	2.36
1	$2.87 \cdot 10^{-2}$	34.8	2.50

The next series of simulations were performed

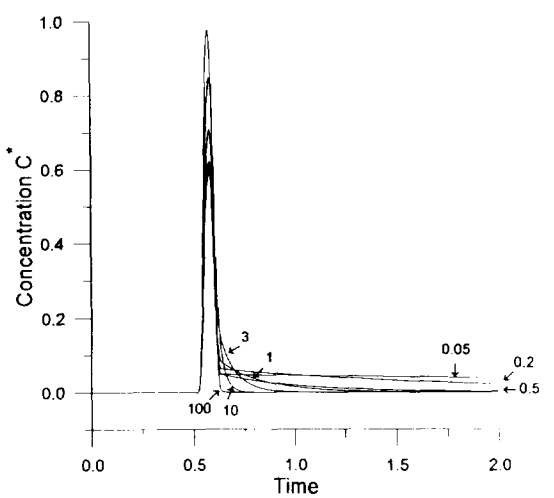

Fig. 1. Influence of desorption coefficient k_d on the apparent concentration profiles c^*; k_d values corresponding to the appropriate profiles are shown by arrows. These results simulate the situation when the sample is diluted or when it is transported by means of a pressure-driven flow.

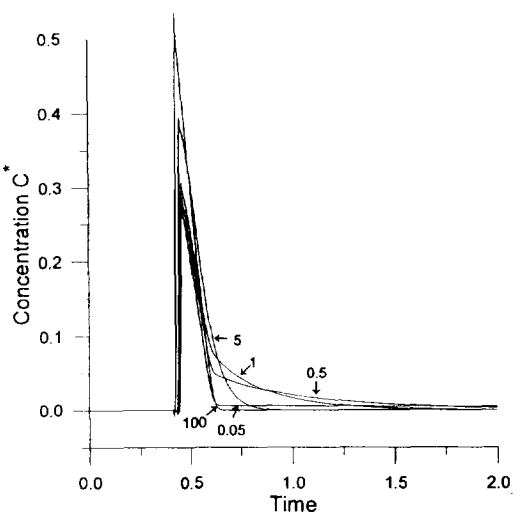

Fig. 2. Influence of desorption coefficient k_d on the apparent concentration profiles c^*; k_d values corresponding to the appropriate profiles are shown by arrows. These results simulate an electrophoretic run with a concentrated sample ($\alpha = -0.3$).

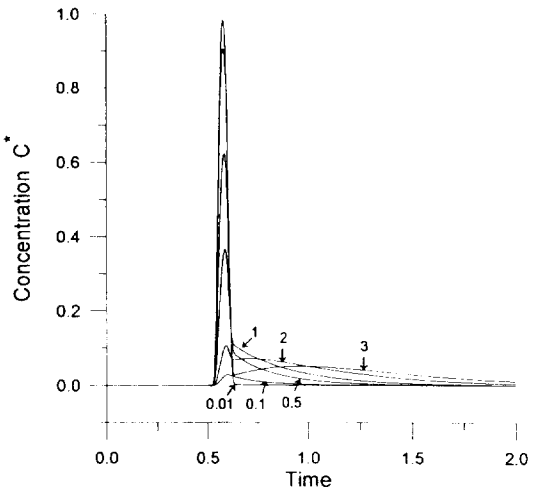

Fig. 3. Impact of wall capacity on the concentration profiles. Concentration profiles corresponding to different parameters S are shown by the arrows. Note peak splitting in profile 3.

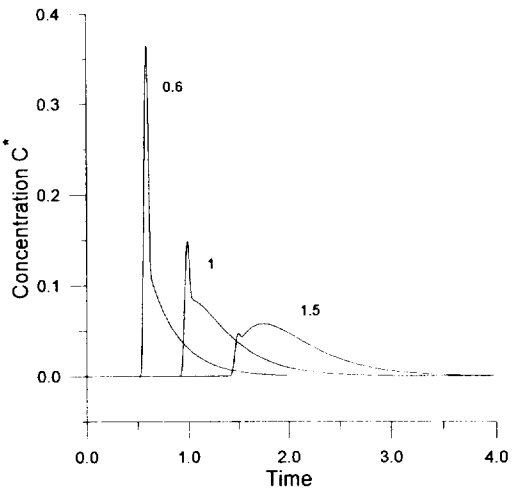

Fig. 4. Simulated profiles for different detector positions (effective capillary length).

for different parameters S, i.e., wall capacity. Simulated profiles are presented in Fig. 3. Only at very small S (0.01) the sample interaction with the wall does not produce a significant effect. At $S \geq 0.1$, the adsorption leads to strongly tailing profiles, the height of the tail depending on the wall capacity, with its length depending on the desorption rate. When the capacity of the wall is very large ($S = 3$), the sample electropherogram in fact has two peaks, the first due to the sample remaining in solution and the second caused by desorption processes. The relationship between Sk_a and k_d is such that the desorption process combined with electrophoretic migration gives the second concentration wave. In the limiting case $S \rightarrow \infty$ the sample never reaches the detector since it will be adsorbed at the beginning of the capillary.

Similar results are observed on modelling different capillary lengths by shifting the detector position. The simulated electropherograms are plotted in Fig. 4. If the effective capillary length is relatively large ($x_{det} = 1.5$), the sample peak given by the substance in solution becomes small (one should remember that the concentration profiles plotted represent the sum of the sample concentration in solution and that on the wall) while the second larger peak is created by the substance attached to the wall. As the sorption process takes some time, the second peak moves more slowly.

The results of wall adsorption for four initial sample concentrations are presented in Fig. 5. As can be seen, the loss of sample due to its binding is proportional to its initial concentration. However, the desorption process is faster for higher concentrations also, so the relative

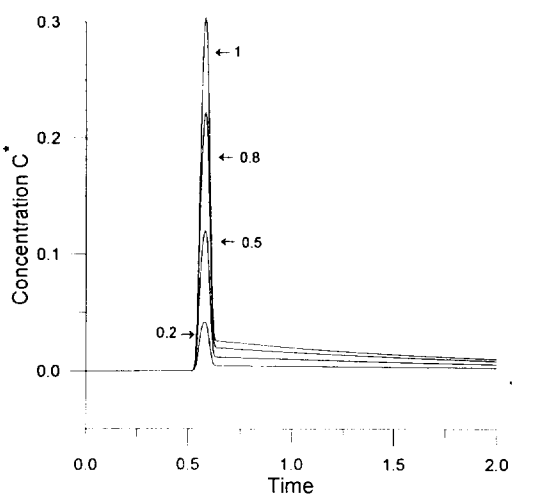

Fig. 5. Apparent concentration profiles for different initial sample concentrations.

loss in peak height and number of theoretical plates is greater for low concentrations.

4.2. Experiments

For the sake of simplicity, the studies on ionic interaction with the wall were started with monovalent positively charged substances at buffer pH values of 5–9. Under these conditions, the wall in an uncoated capillary should be negatively charged, so one could expect a strong ionic interaction of the sample with the wall. However, experiments with small ions showed the opposite situation, i.e., weak wall–sample interaction, as described below. Pyridine at a concentration of 5 m*M* was run in 20 m*M* acetate buffer titrated with NaOH to pH 5. This run was then simulated using the approach analogous to that in Ref. [33] in which the sample interaction with the wall is neglected. The experimental and calculated profiles of pyridine concentration are plotted in Fig. 6. The shape of the experimental peak is similar to the simulated one and the baseline returns to its previous level, which indicates weak adsorption, if any. The other proof is the absence of sample mass losses due to attachment to the wall during its migration along the capillary. The discrepancy in the substance mass contained in each of these peaks is approximately 7%, which is a reasonable discrepancy between experiment and simulation [33]. Additional experiments with alkaline Immobiline (N,N-dimethylaminopropylacrylamide, pK = 9.33) [34] also confirmed our hypothesis. Thus for Immobiline (c_0 = 1 m*M*) migrating in 20 m*M* Tris buffer, titrated with HCl to pH 8, we measured the total variance of the sample peak σ_{exp} in the electropherogram and compared it with theoretical estimation σ_t, expressed as [35]

$$\sigma_t^2 = \sigma_{Hi}^2 + \sigma_{diff}^2 + \sigma_i^2 = \frac{\Delta P^2 r_0^6 t_{inj}}{1536\eta^2 l^2 D} + 2Dt_{mig} + \frac{h^2}{12}$$

where ΔP, t_{inj}, η, l, t_{mig} and h are injection pressure, time of injection, buffer viscosity, capillary length, migration time and sample plug length, respectively. The first term in this sum describes the dispersion due to the parabolic flow profile during sample loading, the second accounts for diffusion dispersion and the third the variance due to the finite sample length. In an experiment in which $\sigma_{exp} = 4.3 \cdot 10^{-6}$, the theoretical value $\sigma_t = 3.71 \cdot 10^{-6}$, which is close to the first one, and the difference between these two values does not exceed 15% of the total variance. If it is completely ascribed to wall interaction then, according to the equation [26,35]

$$\sigma_{wall}^2 = \frac{C_m r_0^2 v^2 t}{D}, \quad C_m = \frac{k'^2}{4(k'+1)^2}$$

where v is the sample velocity and t the migration time, it will give an estimated wall capacity factor of only k' = 0.078, which is small for small ions. An experiment with a more concentrated sample (10 m*M*) also did not reveal a significant interaction. The absorbance profile of 10 m*M* Immobiline migrating in 10 m*M* phosphate buffer titrated with Tris to pH 7 is plotted as the dashed line in Fig. 6. Owing to variations in conductivity, the shape of the peak is no longer Gaussian, but has a characteristic triangular shape with a sharp rear boundary. In the case of strong sample adsorption it would have a tail of substance being released from the wall. From the above experiments, one can suggest that the small cations, even if they interact with the

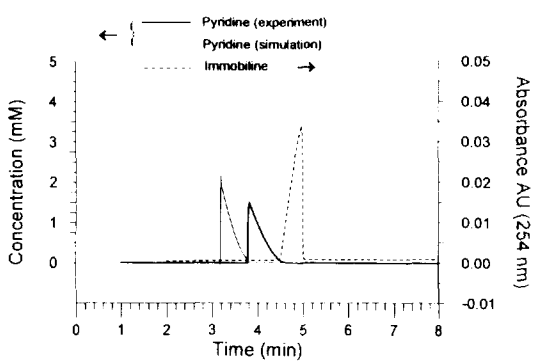

Fig. 6. Concentration profiles of pyridine (experimental and simulated) and absorbance profile of Immobiline. For pyridine the concentration axis is to the left and for Immobiline the absorbance axis is to the right. For explanations, see also text.

capillary wall, are not greatly adsorbed by the wall.

The experiments with biopolymers demonstrate a stronger interaction with the wall compared with small monovalent molecules. A series of experiments were performed with poly-L-histidine (polycation). Some were performed at different pH values for both the electrophoretic and pressure migration modes (Fig. 7). These experiments supported the hypothesis that the sample interaction with the wall is electrostatic in nature, that is, it depends on the degree of silanol ionization. At pH 3, when the capillary wall is almost electrically neutral, the adsorption in both modes is small. After the peak passage the baseline returns to its previous value, so there is no sample attached to the wall. In contrast, at pH 4 and 5, the baseline is shifted after peak passage, suggesting that it is higher at pH 5, when the ionization of the wall is stronger. At a given pH value, the elevation of the baseline is approximately the same for both pressure and electrophoretic runs, which means that the adsorption depends weakly on the sample migration mode.

It is known that at a given buffer pH the capillary wall can be activated by washing with a strong base, e.g., NaOH. The activation assumes that there are more binding centres. This effect is demonstrated by Fig. 8, where poly-L-histidine electropherograms are plotted: two of them correspond to the runs just after the NaOH wash (dashed lines) and the other two after capillary equilibration (solid lines). In the first case the baseline is higher after the peak passage, suggesting that more sample is bound to the wall. This is confirmed also by the sample peak height and area, which are lower in the case of capillary washing with NaOH, since more sample mass is lost before it reaches the detector. It is worth noting that after capillary washing with a strong base it takes several runs to saturate the capillary. We performed eight consecutive runs with poly-L-histidine as a sample before the concentration profiles reached their limiting shape, i.e. did not change from run to run. In fact, the capillary inner surface was covered with the

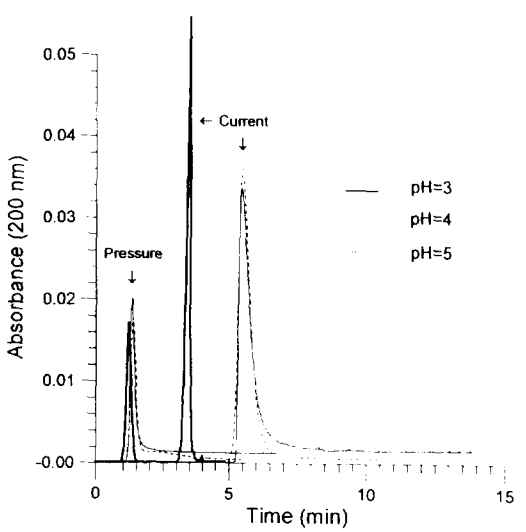

Fig. 7. Poly-L-histidine electropherograms at different values of buffer pH (3, 4 and 5). Sample concentration, 0.5 mg/ml; injection for 2 s by excess pressure; buffer 20 m*M* acetic acid titrated with NaOH. The graphs corresponding to the pressure run and to the electrophoretic run are indicated by arrows.

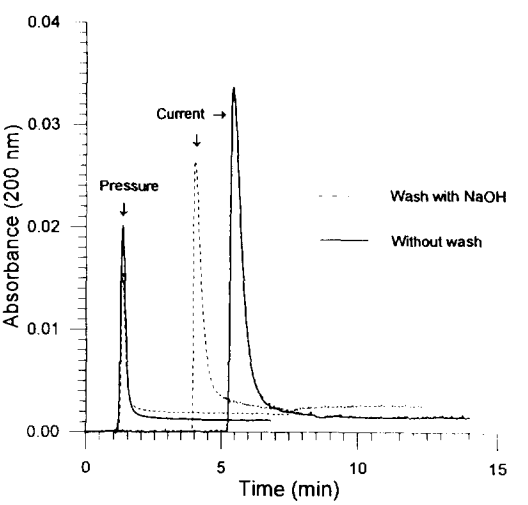

Fig. 8. Influence of NaOH wash (1 *M* NaOH for 5 min, H_2O for 10 min, buffer for 10 min) on the intensity of sample–wall interaction. Sample concentration, 0.5 mg/ml; injection for 2 s by excess pressure; buffer, 20 m*M* acetic acid titrated to pH 5 with NaOH. The graphs corresponding to the pressure run and electrophoretic run are indicated by arrows.

sample, so that at the end the net wall charge was not negative but positive since the electroosmotic flow had changed its direction. This is also visible from Fig. 8, in which the electrophoretically driven sample in a saturated capillary (solid line) has a longer migration time than that immediately after NaOH washing (dashed line).

However, the secondary interaction of poly-L-histidine with the wall still exists even in a saturated capillary, as the baseline does not return to its original level. This means that, besides ionic interactions, other mechanisms of sample binding exist. It has been pointed out [36] that there is a probability of sample–sample interaction, i.e., the sample in solution is bound to the sample stacked on the wall. We suggest two mechanisms: interaction by means of hydrogen bonds and hydrophobic interaction. To verify these hypotheses, we performed similar experiments, but in the presence of 6 *M* urea in the buffer solution in order to break the hydrogen bonds or of 2% Tween-20. The results of both experiments support the first hypothesis, i.e., that the secondary interaction was probably due to the formation of hydrogen bonds. In the presence of urea the baseline returned to its original value, whereas in the presence of Tween-20 it did not (Fig. 9).

The influence of the initial sample concentration on its profile is illustrated by Fig. 10. Three different samples with concentrations c_0 = 0.5, 0.25 and 0.1 mg/ml of poly-L-histidine were applied during pressure runs. The amount of sample bound to the wall was essentially the same in all these runs as the baseline was shifted after the sample peaks by approximately the same value. A possible explanation is that interaction does not depend on the sample concentration, at least when it exceeds some critical value (here it could be a concentration corresponding to this base level shift, which probably represents saturation of the wall binding capacity).

The sample loss during its motion in the capillary could be estimated by carrying out experiments with capillaries of different lengths or putting several detectors along the capillary

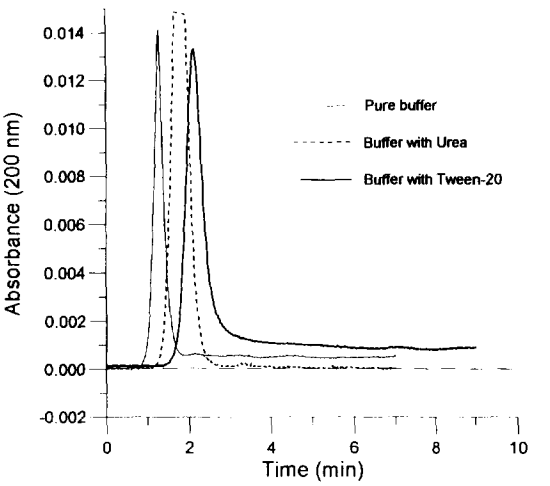

Fig. 9. Influence of urea (6 *M* solution) and Tween-20 in the buffer solution on a secondary sample interaction during a pressure run. Sample concentration, 0.5 mg/ml; buffer, 20 m*M* acetic acid titrated to pH 5 with NaOH; sample injection time, 2 s for plain buffer and a buffer with Tween-20, and 10 s in the experiment with urea, during which more sample was injected. Even under these conditions the lower interaction in the presence of urea is visible.

length, as was done by Towns and Regnier [18]. When working with different capillaries there is a possibility that their properties may vary from

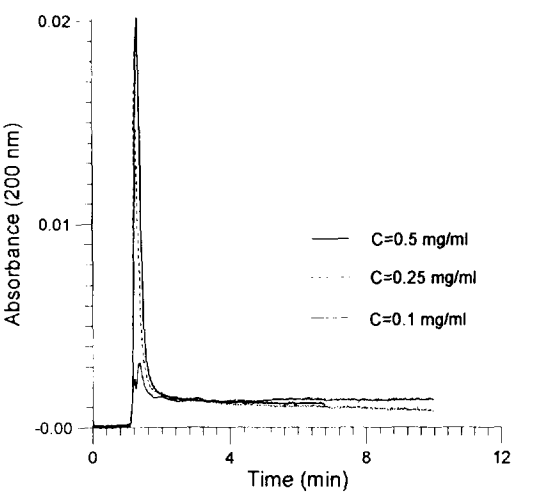

Fig. 10. Absorbance profiles for three different initial concentrations of poly-L-histidine (0.5, 0.25 and 0.1 mg/ml) in a pressure run; injection by pressure (2 s); buffer, 20 m*M* acetic acid titrated to pH 5 with NaOH.

one to another, so we performed these experiments using only one capillary. We used a commercial capillary zone electrophoresis (CZE) unit for our experiments which has only one detector, so we injected the sample from the opposite ends of the capillary. In one case the migration length was around 19.4 cm and in the other one it was 6.8 cm. First, the experiment was performed on a saturated capillary, which was equilibrated with the sample for a long time in order to minimize the sample interaction. In this case the injection was performed from the detector end. Then the capillary was washed with 1 *M* NaOH solution and experiments were repeated by injecting the sample from both capillary ends. Three electropherograms corresponding to these experiments are plotted in Fig. 11. Assuming that in the case of a saturated capillary the sample mass was not lost before detection, one can estimate the amount of sample which has been lost in the consecutive runs when the adsorption was strong. Then, according to this information, we could estimate also how

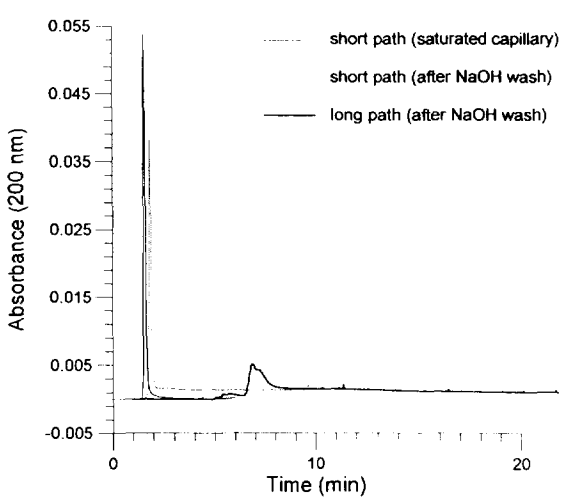

Fig. 11. Influence of capillary length and detector position on the sample profile. Two profiles: the dashed line and thin solid line correspond to a short capillary (6.8 cm); the thick line corresponds to a longer capillary (19.4 cm). In one experiment the capillary wall was saturated (thin solid line) and in the other two the experiment was preceded by an NaOH wash. Sample (poly-L-histidine) concentration, 0.5 mg/ml; buffer, 20 m*M* acetic acid titrated to pH 5 with NaOH.

well the poly-L-histidine sample covers the silanol groups. The number of silanol groups per 1 cm of capillary length, N_{Si}, could be estimated knowing the capillary radius $r_0 = 37.5 \cdot 10^{-4}$ cm and the density of silanols $n_{Si} \approx 5 \cdot 10^{14}$ cm^{-2} [37], $N^0_{Si} = 2\pi r_0 n_{Si} \approx 1.18 \cdot 10^{13}$ groups/cm. In all experiments presented in Fig. 11 the initial concentration of poly-L-histidine was 0.5 mg/ml and the injection volume was $1.14 \cdot 10^{-5}$ ml. Calculating the area of the peaks, rough estimates give a value for the loss of sample due to its interaction with the wall per 1 cm of capillary of $m = 3 \cdot 10^{-7}$ mg/cm. According to this, the upper limit of active binding centres able to interact with the wall is $N^0_{his} = (m/\mu_{his})N_A \approx 1.2 \cdot 10^{12}$ groups/cm, where μ_{his} is the molecular mass of histidine and N_A is Avogadro's number. Taking into account the degree of ionization of silanol ($pK_{Si} = 6.3$) [38] and poly-L-histidine with a pK value equal to that of the free base ($pK_{his} = 6.0$) [39] in buffer with pH 5, the corrected values would be $N_{Si} = N^0_{Si}K_{Si}/(H + K_{Si}) = 5.6 \cdot 10^{11}$ groups/cm and $N_{his} = N^0_{his}H/(H + K_{his}) = 10.9 \cdot 10^{11}$ groups/cm. The estimated values show that they are of the same order of magnitude, which means that the capillary wall is completely covered with the sample.

A series of experiments were performed in order to investigate the influence of ionic strength on sample interaction. For this purpose we used pressure runs, since in this case there are no problems due to an increase in current and heat dissipation [11]. The experiments were performed with cytochrome *c* as a sample in 20 m*M* CAPS buffer titrated with NaOH to pH 10. Different amounts of salt (NaCl) were added to the buffer, so its concentration was 50, 100 and 200 m*M*. The experimental electropherograms are plotted in Fig. 12, together with the case in which no salt was added. It is clearly visible that an increase in salt concentration suppresses the sample–wall interaction significantly. The shift of the baseline after 8 min is close to zero at salt concentrations 50 and 100 m*M*, in contrast to the case with zero salt concentration. At a salt concentration of 100 m*M* the sample tail is much smaller than that at 50 m*M*, which means that the interaction is lower; however, the difference

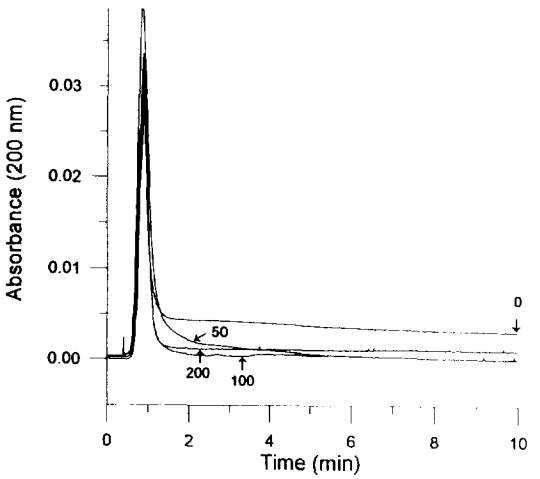

Fig. 12. Influence of ionic strength on sample–wall interaction. Buffer, 20 m*M* CAPS–NaOH (pH 10); sample, 1 mg/ml cytochrome *c*. The difference in ionic strength was created by addition of various concentrations of salt (NaCl): 0, 50, 100 and 200 m*M*.

in profiles between 100 and 200 m*M* salt is so small that a further increase in salt concentration does not produce a significant effect.

5. Discussion

Two obvious features which govern the wall adsorption process in a capillary are the capacity of the wall, which is connected with the density of active binding centres on its surface, and the interaction kinetics, which are responsible for the rate of exchange of sample between the solution and the wall. When studying ionic interactions, we assume that the capacity of the wall is associated with the charge density on it, due to silanol ionization. We also assume that the higher is the charge density, the greater is the number of binding centres and the higher is the capacity of the wall and hence interaction and adsorption (see Fig. 3). This is also in accordance with experimental data, which show that, with an increase in the charge density on the wall, the interaction is enhanced (Figs. 7 and 8). By increasing the pH of the buffer, the charge density on the wall is increased in addition to the sample interaction (Fig. 7). Another way to increase the capacity of the wall is to wash it with a strong base (1 *M* NaOH), as presented in Fig. 8.

The factors influencing the sorption kinetics are not so obvious. First it is unclear why small monovalent cations (pyridine, Immobiline) do not exhibit strong adsorption, while the polycations (poly-L-histidine) and proteins (cytochrome *c*) do. There have been several studies on the influence of cations, including small cations of alkali and bivalent metals, on electroosmotic flow [11,40,41]. It was shown [40,41] that alkali metals are fairly effective in quenching the electroosmotic flow, the large-sized cations being more effective than small cations. The most probable explanation of this phenomenon is that larger cations are adsorbed on the capillary wall, thereby altering its charge and reducing the electroosmotic ζ-potential. Similar results were also obtained by Green and Jorgenson [11], who used alkali metal cations for minimizing protein adsorption on bare silica. A series of amines are listed in Ref. [42], which, when added to the background electrolyte (at concentrations up to 10 m*M*), markedly helped in stabilizing the electroosmotic flow (EOF) (improving the precision of migration times to better than 1%). All this means that small cations interact with the capillary wall and could significantly change its properties. However, in our case, it seems that the ionic interaction of small cations does not lead to strong adsorption (see Fig. 6) because, we assume this interaction has a dynamic character. We propose the following qualitative explanation of this phenomenon. The small cations are able to be bound by means of one (or very few) points to the few active binding centres on the capillary wall, whereas for the polyvalent molecule the points of binding may be numerous [43]. For each binding contact due to ionic interaction, the probability to be bound P_b is between zero and unity, $0 < P_b < 1$, where $P_b = 0$ corresponds to the absence of interaction and $P_b = 1$ means irreversible binding to the wall. Hence the probability of being free from such binding contact is also less than unity, $P_f < 1$. For monovalent molecules the probability of being bound or of staying in solution coincides

with P_b and P_f, respectively. However, for polycations, if we assume that one act of binding in one part of the molecule occurs independently of the other similar acts in the other parts of the same molecule, the probability P of being free is the product of n factors P_f, i.e.,

$$P = \underbrace{P_f \cdot P_f \cdot \ldots P_f}_{n \text{ times}} = P_f^n$$

where n is the number of binding centres in the molecule. This means that the probability of being free for a large molecule is much less than for a small molecule. For example, if $P_f = 0.9$, for a polybase with a number of bases $n = 50$, it will be $P = (0.9)^{50} = 0.0052$, i.e., the molecule will stay attached to the wall all the time. In this case the desorption kinetics are very slow. Of course, in reality, everything is much more complicated, but this could give an idea of what happens with large molecules.

The probability of being bound to the wall depends on the presence of different co-ions in buffer solution, which can compete with sample ions. Here again we assume an ionic mechanism of interaction between cations in solution and a negatively charged capillary wall. The higher the concentration of competing ions, the lower is the probability of a sample being bound and the faster are its desorption kinetics. This was observed when salt was added to the buffer and the Na^+ ions competed with the positively charged parts of the cytochrome c molecule in binding to the wall (Fig. 12). Thus, by adding salts to the buffer solution, the desorption rate was increased, which led to a decrease in tailing phenomena (compare Figs. 1 and 12). The sorption kinetics also depend on the charge density on the capillary wall and the degree of ionization of sample species. Thus, on going from a low to a higher buffer pH, in concomitance with an increment of wall capacity, the desorption kinetics also change (decrease, see Fig. 7).

Among other interesting features found in the experimental and simulated data is the existence of two peaks in the electropherograms when the interaction of the sample with the wall was strong and a significant part of it was adsorbed before it reached the detector (compare Fig. 10, $c_0 = 0.1$, Fig. 4, $x_{det} = 1.5$, and Fig. 3, $S = 3$). According to the simulation, the first peak is given by the substance moving in solution by means of an external force whereas the second is caused by a desorption wave. It is initiated by a concentration drop in solution immediately after the passage of the first peak.

However, in some cases the mathematical model is not fully adequate for the phenomena described and could give wrong predictions. Thus the experiments with different initial sample concentrations gave approximately the same sample tail (Fig. 10). The shift of the baseline was equal in all cases, whereas in simulations it depended on the sample concentrations (Fig. 5).

Of course, this model is a very simple one and it could not pretend to describe all details of sample evolution in a capillary. First it is not clear how valid is the assumption on Langmuir-type kinetics applied to the wall adsorption process. Probably other kinetic models should be tried to find a better correspondence. The next step, for a more accurate description, is to consider the sample transport in solution in the radial direction, i.e., to solve a two-dimensional problem.

6. Conclusions

In the course of our continuing research on analyte–capillary wall interactions during CZE, we have presented a mathematical model based on non-linear equilibrium chromatography coupled to sample desorption from the wall essentially by diffusional processes. The present semi-quantitative mathematical model, although far from being immune from failures, can describe several phenomena of analyte binding to the capillary wall. An effective indicator is the overall peak shape, including its symmetry, height and total area. For example, loss of peak height and total area suggests sample mass loss due to irreversible adsorption on the wall. Conversely, maintenance of peak symmetry (in the absence of a mismatch between sample and electrolyte conductivities), and a return to the baseline after

the peak wave are clear indicators of the absence of sample binding to the wall (or, as a first approximation, of fast desorption kinetics compared with the electrophoretic sample velocity). Our observations have additionally given support to a well known phenomenon in CZE that preconditioning of the capillary with strong bases, even at constant pH, results in activation of the capillary surface and augmentation of sample adsorption on it. In fact, polycation adsorption, as evidenced by higher baseline levels after the peak shock, is markedly increased.

Our modelling can predict a variety of scenarios occurring in a CZE run. Perhaps most notable among them is the splitting of a homogeneous analyte into two peaks as a result of an equilibrium between bound and unbound sample at the injection port, at appropriate wall charge densities. On the experimental side, we find that polycations are adsorbed on the capillary wall, at any pH above 3, into multiple strata until electroosmotic flow reversal (as reported by a number of workers, e.g., [18]). In our case, however, this layering process is more probably driven by H-bond formation than by hydrophobic interaction among neutralized chains, since it is very sensitive to 6 *M* urea but essentially unaffected by the presence of surfactants (e.g., Tween-20).

Acknowledgements

This work was supported in part by grants from the Comitati di Chimica e Biologia e Medicina (CNR, Rome) and by the Radius in Biotechnology (ESA, Paris). L. Capelli is the winner of a fellowship from Italy's National Research Council (CNR).

References

[1] J.W. Jorgenson and K.D. Lukacs, *Anal. Chem.*, 53 (1981) 1298–1302.
[2] S.F.Y. Li, *Capillary Electrophoresis*, Elsevier, Amsterdam, 1992.
[3] C.T. Wu, T.-L. Huang and C.S. Lee, *Anal. Chem.*, 65 (1993) 568–571.
[4] X. Huang, M.A. Quesada and R.A. Mathies, *Anal. Chem.*, 64 (1992) 967.
[5] C.T. Culbertstone and J.W. Jorgenson, *Anal. Chem.*, 66 (1994) 955–962.
[6] F.E. Regnier and D. Wu, in N.A. Guzman (Editor), *Capillary Electrophoresis Technology*, Marcel Dekker, New York, 1993, pp. 287–309.
[7] S. Hjertén, *Chromatogr. Rev.*, 9 (1967) 122–219.
[8] G.J.M. Bruin, J.P. Chang, R.H. Kuhlman, K. Zegers, J.C. Kraak and H. Poppe, *J. Chromatogr.*, 471 (1989) 429–436.
[9] W. Nashabeh and Z. El Rassi, *J. Chromatogr.*, 559 (1991) 367–383.
[10] S. Hjertén, *J. Chromatogr.*, 347 (1985) 191–198.
[11] J.S. Green and J.W. Jorgenson, *J. Chromatogr.*, 478 (1989) 63–70.
[12] J.H. Jumppanen, H. Sirèn and M.L. Riekkola, *J. High Resolut. Chromatogr.*, in press.
[13] H.H. Lauer and D. McManigill, *Anal. Chem.*, 58 (1986) 166–170.
[14] M.M. Bushey and J.W. Jorgenson, *J. Chromatogr.*, 480 (1989) 301–310.
[15] C.S. Lee, W.C. Blanchard and C.T. Wu, *Anal. Chem.*, 62 (1990) 1550–1552.
[16] M.A. Hayes, I. Kheterpal and A.G. Ewing, *Anal. Chem.*, 65 (1993) 2010–2013.
[17] Z. Zhao, A. Malik and M.L. Lee, *Anal. Chem.*, 65 (1993) 2747–2752.
[18] J.K. Towns and F.E. Regnier, *Anal. Chem.*, 64 (1992) 2473–2478.
[19] L.G. Öfverstedt, G. Johansson, G. Fröman and S. Hjertén, *Electrophoresis*, 2 (1981) 168–173.
[20] E. Grushka, in F. Dondi and G. Guiochon (Editors), *Theoretical Advancement in Chromatography and Related Separation Techniques*, Kluwer, Dordrecht, 1992, pp. 607–632.
[21] M.R. Schure and A.M. Lenhoff, *Anal. Chem.*, 65 (1993) 3024–3037.
[22] J.L. Wade, A.F. Bergold and P.W. Carr *Anal. Chem.*, 59 (1987) 1286–1295.
[23] G. Guiochon, S. Golshan-Shirazi and A. Jaulmes, *Anal. Chem.*, 60 (1988) 1856–1866.
[24] S. Golshan-Shirazi and G. Guiochon, *J. Chromatogr.*, 506 (1990) 495–545.
[25] S. Hjertén, *Electrophoresis*, 11 (1990) 665–690.
[26] J.P. McEldon and R. Datta, *Anal. Chem.*, 64 (1992) 227–230.
[27] E. Grushka, in N. Catsimpoolas (Editor), *Methods of Protein Separation*, Vol. I, Plenum Press, New York, 1975, Ch. 6, pp. 161–192.
[28] G. Taylor, *Proc. R. Soc. London, Ser. A*, 219 (1953) 186–203.
[29] R. Aris, *Proc. R. Soc. London, Ser. A*, 235 (1956) 67–77.
[30] S.V. Ermakov, O.S. Mazhorova and Yu.P. Popov, *Informatica*, 3 (1992) 173–197.

[31] S.V. Ermakov, M.S. Bello and P.G. Righetti, *J. Chromatogr. A*, 661 (1994) 265–278.
[32] C.A.J. Fletcher, *Computational Techniques for Fluid Dynamics 1, Fundamental and General Techniques*, Springer, Berlin, 1988.
[33] S.V. Ermakov and P.G. Righetti, *J. Chromatogr. A*, 667 (1994) 257–270.
[34] M. Chiari and P.G. Righetti, *Electrophoresis*, 13 (1992) 187–191.
[35] P.D. Grossman, in P.D. Grossman and J.C. Colburn (Editors), *Capillary Electrophoresis. Theory and Practice*, Academic Press, San Diego, 1992, Ch. 1, pp. 3–43.
[36] M. Diack and G. Guiochon, *Anal. Chem.*, 63 (1991) 2608–2613.
[37] K.K. Unger, *Packing and Stationary Phases in Chromatographic Techniques*, Marcel Dekker, New York, 1979.
[38] T.L. Huang, P. Tsai, G.T. Wu and C.S. Lee, *Anal. Chem.*, 65 (1993) 2887–2893.
[39] R.C. Weast (Editor), *CRC Handbook of Chemistry and Physics*, CRC Press, Boca Raton, FL., 67th ed., 1987, pp. D159–D161.
[40] I.Z. Atamna, H.J. Issaq, G.M. Muschik and G.M. Janini, *J. Chromatogr.*, 588 (1991) 315.
[41] H.J. Issaq, I.Z. Atamna, G.M. Muschik and G.M. Janini, *Chromatographia*, 32 (1991) 155.
[42] N. Cohen and E. Grushka, *J. Chromatogr. A*, 678 (1994) 167–175.
[43] F.E. Regnier and K.M. Gooding, in E. Heftman (Editor), *Chromatography, Part B: Applications*, Elsevier, Amsterdam, 5th ed., 1992, Ch. 14, pp. B151–B169.